Weather types and rainfall variability during the Northeast Monsoon over Malaysia

Xia Yan New[1], Juneng Liew[1,2], Tangang Fredolin[3]

[1] Department of Earth Sciences and Environment, Faculty of Science and Technology, Universiti Kebangsaan Malaysia, Bangi, Selangor, Malaysia.

[2] Centre for Tropical Climate Change System (IKLIM), Institute of Climate Change, Universiti Kebangsaan Malaysia

[3] Geography, Environment and Development (GED) Programme, Faculty of Arts and Social Sciences (FASS), Universiti Brunei Darussalam, Jalan Tungku Link, Brunei Darussalam.

*Corresponding Author

Email: juneng@ukm.edu.my

Keywords:

1. Northeast Monsoon
2. Synoptic Circulation
3. Weather Types
4. Cold Surge
5. Borneo Vortex
6. Rainfall Distribution

Abstract

Malaysia frequently experiences extreme rainfall throughout the Northeast Monsoon season. However, the connection between extreme rainfall and distinct monsoonal synoptic circulations remains to be fully investigated. This study aims to identify the dominant synoptic circulation patterns and the associated extreme precipitation using weather type classification method. K-means algorithm was employed to classify daily weather types (WTs) over Malaysia region (3°S–10°N, 98°–122°E) during Northeast Monsoon season, which occurring from November to February. The classification was based on 850-hPa wind data obtained from the fifth generation of the European Centre for Medium-Range Weather Forecasts (ECMWF) Reanalysis v5 (ERA5) dataset from 1981 to 2020. Four distinct WTs were identified and further examined their circulation pattern, frequency of occurrence, typical progression and persistence, and associated rainfall characteristics. Among the identified synoptic circulation patterns, the Borneo Vortex, cold surge, and cross-equatorial surge were prominent within the resultant WTs. Over the past 40 years, the co-occurrence of Borneo Vortex and cold surges has shown a significant decrease trend, while the other three patterns, including the Borneo Vortex occurring over South China Sea, weak cold surges, and cross-equatorial surges have exhibited increasing trends. The cold surges contribute to increased rainfall in western Borneo, particularly in the Sarawak region. The occurrence of the Borneo Vortex leads to increased rainfall in eastern Borneo, while cross-equatorial surges are associated with enhanced rainfall in northeastern Borneo. Lastly, this study look into how El Niño–Southern Oscillation (ENSO) modulates the occurrence of each of the four WTs. Borneo Vortex events occur more frequently during La Niña years compared to El Niño years. As Malaysia continues to face the challenges of climate change, this study helps in developing strategies to manage the risks related to extreme events, helping communities and industries adapt and sustain

resilience.

1. Introduction

Malaysia which located over west of the Maritime Continent experiences a unique climate that influenced by significant seasonal variations throughout the year [1], as well as interannual variations [2-4] and intraseasonal variations [5]. Two distinct monsoon regimes dominate Malaysia's climate: the boreal winter monsoon, known locally as the Northeast Monsoon, is typically associated with wetter conditions, whereas the boreal summer monsoon, known locally as the Southwest Monsoon, is comparatively drier. The period of transition between these two monsoons is referred to as the inter-monsoon phase [6].

The Northeast Monsoon has a significant impact on Malaysia's climate, primarily by triggering convection via interactions with the local sea and land breeze circulation and through the orographic lifting effect [7]. This impact typically dominates from late November to February [6, 8-10], and largely affected areas faces the South China Sea such as Peninsular Malaysia's eastern coast. However, Peninsular Malaysia's west coast can also be affected [11]. During this period, Peninsular Malaysia's east coast areas experience a significant increase in rainfall, with approximately 50% of its annual precipitation occurring at the beginning of the Northeast Monsoon in November and December. In years characterized by active monsoon conditions, this contribution can rise dramatically, with up to 70% of the annual rainfall concentrated within these months [12]. This intensified monsoon rainfall has leads to widespread flooding, resulting in severe mortality, displacement of communities, and damage to infrastructure. Looking ahead, the situation is expected to become even more challenging, as projections indicate that extreme monsoon rainfall is expected to increase in both frequency and intensity resulting from the ongoing impacts of climate change [13-15].

On average, the low-level northeasterly winds during November to February can abruptly intensify into episodes of strong and persistent winds about five to six times a year. This intensification is caused by the strengthening of Siberian High pressure system. This results in a phenomenon called 'cold surge', which is one of the most energetic monsoonal circulation systems [16]. Another prominent circulation feature during the Northeast Monsoon season is the Borneo Vortex [17]. These are the two primary features that dominating low-level circulation patterns over Malaysia on synoptic time scales [5, 10, 16-18]. Cold surges are pulses of strong northeasterly winds propagate across the South China Sea toward Peninsular Malaysia, which is triggered by a strong pressure gradient between the Siberian High and the lower pressures near South China Sea. In addition, the cold surge also enhances the near-surface northeasterly winds that rapidly progress southward, with Malaysia's topography acting as a barrier that channels the flow equatorward. These winds begin as dry flows but gain moisture while traveling across the South China Sea, becoming more humid by the time they reach Malaysia [9, 16]. The Borneo Vortex, is an anti-clockwise mesoscale circulation over Borneo and its surrounding regions. It usually formed through the interaction between shear vorticity induced by northeasterly winds over South China Sea and the relatively weaker winds along the western coast of Borneo [7, 17, 19]. This features has a significant influence on moisture recirculation, and frequently related with intense latent heat release and deep convection [16].

Both of these features are known as the primary drivers of severe weather events near South China Sea region [10, 16]. From December 2006 to late January 2007, the cold surge phenomenon caused one of the century's worst floods near southern Peninsular Malaysia, affecting more than

200,000 residents and resulting in 16 deaths [5]. In addition, as a cold surge travel equatorward and cross the South China Sea, it may interact with the Borneo Vortex, and potentially intensify disturbances through enhanced low-level moisture convergence and organized deep cumulus convection [1, 16]. When these circulations interact with the terrain, it may results in strong convection, as seen in the formation of Typhoon Vamei, which occurred on December 26, 2001 near Singapore [20].

However, the relationship between extreme precipitation and various monsoonal synoptic circulations during the Northeast Monsoon in Malaysia is not fully understood. As noted by [16] and [10], there are various recurring circulations that may affect Malaysia differently. However, how these patterns are influenced by intraseasonal oscillations and interannual variations remains to be fully investigated. [5] highlighted the possible interactions between Madden-Julian Oscillation (MJO) and the cold surges that could intensify moisture convergence in Peninsular Malaysia. Besides that, [4] also indicated that Malaysia experiences severe extreme precipitation events that influenced by both El Niño and La Niña. In addition, [19] have also identified a long-term trend on the cold surge and Borneo Vortex. Hence, a key scientific question is whether different types of recurring low-level circulations exist and can be linked to episodes of extreme precipitation in Malaysia. Hence, the objective of this study is to assess the extent to which rainfall variability is linked to various regional-scale atmospheric circulation patterns using weather types identified through cluster analysis.

Clustering analysis is a type of multivariate statistical technique used to classify daily weather patterns into distinct representative states based on their similarity [21, 22]. By employing weather typing analysis, the dominant weather patterns in a region can be objectively identified. This approach has been utilized in many studies to describe recurrent circulation patterns such as in the North Atlantic [21, 23], North America [24], and Europe [25]. In tropical regions, weather typing analysis has also been employed in studies over East Africa [26], and Indonesia [27]. In order to identify weather patterns, the k-means clustering algorithm is among the most prevalently employed methods [28], which has proven useful in identifying circulation patterns [29, 30]. In addition, weather typing method can be applied to characterize the variations in rainfall anomalies and extreme events [24, 31]. Hence, in this study, weather types are identified using the k-means clustering algorithm, employed to daily low-level 850-hPa winds to investigate the dominant synoptic circulation patterns during the Northeast Monsoon over Malaysia.

This paper proceeds as follows. Section 2 presents the data and methodology, such as the application of the k-means clustering technique to derive WTs in Malaysia during the Northeast Monsoon season. Section 3 presents the findings of the weather typing analysis, examining the identified WTs and their synoptic circulation patterns, frequency of occurrence, typical progression and persistence, associated precipitation characteristics, and their relationship with the El Niño–Southern Oscillation (ENSO). Section 4 concludes the paper by summarizing the key findings and highlights gaps for future studies.

2. Data and Methods

2.1. Study Area and Data

The first step of this study involves identifying and extracting the dominant WTs over Malaysia. To achieve this, the analysis focuses on a domain extending from 3°S to 10°N in latitude and from 98°E to 122°E in longitude, as illustrated in Fig 1. This region was selected because it is sufficiently large to capture key atmospheric circulation features near Malaysia, ensuring a comprehensive representation of regional atmospheric variability. For example, Borneo Vortex has been reported to occur within the area of 107.5°E–117.5°E and 2.5°S–7.5°N [16, 19], which falls within the area used in this study. Besides that, this study concentrates on the months from November to February during the period 1981 to 2020, coinciding with the Northeast Monsoon season, which is the main period for extreme rainfall in Malaysia.

Fig 1. Study domain. The larger box encompassing Malaysia and nearby land areas. The smaller box represents the region selected as input for the k-means clustering algorithm, which was applied to identify the dominant weather types.

The atmospheric data used for k-means clustering is consist of the daily 850-hPa zonal (u) and meridional (y) component winds, which obtained from the Fifth Generation European Centre for Medium-Range Weather Forecasts (ECMWF) Reanalysis v5 (ERA5) dataset, provided by Copernicus Climate Change Service (C3S) [32]. The 850-hPa level is selected due to its effectiveness in representing monsoonal circulation in tropical regions and its widespread use in previous studies [27]. These wind fields are particularly relevant for analyzing the large-scale flow patterns that govern monsoonal weather systems. For example, Hassim and Timbal [33] used 850-hPa wind data to characterize monsoonal weather types in Singapore and the broader Maritime Continent. The frequent application of 850-hPa winds in such studies highlights their effectiveness in capturing key atmospheric circulations during Northeast Monsoon seasons over Malaysia. Furthermore, 850-hPa winds are considered effective for identifying synoptic-scale disturbances, such as cold surge index, which is based on the daily area-averaged wind speed at this pressure level [16].

The rainfall data used cover the same period, which is from November to February from 1981 to 2020, and are sourced from the gridded precipitation dataset provided by the Climate Hazards Group InfraRed Precipitation with Station data (CHIRPS). This dataset is openly accessible online at https://data.chc.ucsb.edu/products/CHIRPS-2.0/global_daily/. CHIRPS offers high-resolution rainfall data at a spatial resolution of 0.05° × 0.05° [34]. This rainfall dataset has been evaluated for use in Malaysia [35] and recently used by Zakaria et al. [36] for drought evaluation in Malaysia.

In addition to analyzing rainfall variability, this study also examines the influence of ENSO variations on the occurrence of WTs. For this purpose, the Oceanic Niño Index (ONI) is used. The ONI dataset is obtained from the Climate Prediction Center (CPC) of the National Oceanic and Atmospheric Administration (NOAA) and can be accessed at https://origin.cpc.ncep.noaa.gov/products/analysis_monitoring/ensostuff/ONI_v5.php.

2.2. K-means clustering method

To determine the dominant WTs over Malaysia, k-means algorithm was applied to the daily low-level wind data at 850-hPa level, following the methodologies by [37] and [23]. Before conducting the k-means analysis, standardization of the wind dataset was performed. To standardize the wind dataset, the climatological daily mean was removed and the result was divided by the climatological daily standard deviation, giving values with zero mean and unit variance. Standardizing the data before conducting Empirical Orthogonal Function (EOF) analysis enables small-scale wind field fluctuations comparable to large-scale circulation patterns. The standardized anomalies of the 850-hPa u and v wind components were then subjected to EOF analysis, retaining

90% of the total variance in the combined matrix. This dimensionality reduction step decreases the degrees of freedom and enhances computational efficiency. The resulting transformed dataset, structured as an $nt \times ns$ matrix, was then subjected to k-means clustering to objectively classify the dominant WTs.

By minimizing the within-cluster variance, the k-means clustering algorithm is intended to separate the dataset into a predetermined number of clusters, k, denoted as the function W. The purpose is to find the smallest value of $W(P)$, where P indicates the partitioning of the data. The function is defined in equation 1 below:

$$W(P) = \sum_{j=1}^{N} \sum_{x \in C_j} d^2(X, Y_j) \quad (1)$$

P represents a specific grouping of the data, where all-days data was grouped into k clusters $C_1, C_2, \cdots, C_k$. Each cluster C_j has a centroid of Y_j. The distance between a data point X in cluster C_j and its centroid Y_j is measured using squared Euclidean distance $d^2(X, Y_j)$, which reflects how similar data point X to its centroid.

The function $W(P)$ represents the intra-cluster sum of variances for a given partition P. The optimal partition is the one that minimizes $W(P)$. The process of minimizing $W(P)$ provides the optimal division of the data into k clusters. This minimization is carried out iteratively and made more efficient by selecting new centroids from a new subset of the data.

2.3. Determination of the optimal number of clusters

The ideal number of clusters k needed to achieve an adequate amount of separation of the data can be determined using the classifiability index (CI) [23, 24]. The CI is obtained based on anomaly correlation coefficients (ACC) of the partitioned clusters. Equation 2 below has defined the ACC between two partition clusters P_i and Q_j:

$$ACC\left(P_i , Q_j\right) = \frac{\sum_{n=1}^{N} p'_n q'_n}{\sqrt{\sum_{N=1}^{N} (p'_n)^2 \sum_{n=1}^{N} (q'_n)^2}} \quad (2)$$

$$p'_n = p_n - \frac{\sum_{n=1}^{N} p_n}{N}$$

and

$$q'_n = q_n - \frac{\sum_{n=1}^{N} q_n}{N}$$

In this context, $1 \leq i, j \leq k$, with $P \neq Q$. The terms p_n and q_n indicate the cluster's centroid belonging to partitions P_i and Q_j respectively. Accordingly, ACC value will be ranges from -1 to 1, where ACC = 1 suggests that two partitioned clusters are identical to one another. Following [27], each cluster P_i is assigned an ACC score. Each of the ACC score is determined by averaging the highest ACC values between P_i and every cluster Q_j, across partitions where $Q \neq P$, with $j = 1, \ldots, k$. Given N partitions, this results in $N \times k$ ACC scores. Thus, the partition achieving the highest ACC score is regarded as offering the optimal division of the data into k clusters. The value of CI is then computed by averaging the ACC scores across all partitions. The CI is evaluated for different values of k for determining the ideal number of clusters needed.

The statistical significance of the CI values is examined by repeatedly applying the k-means algorithm to datasets constructed from randomly generated red noise. This approach provides a baseline against which the observed CI values can be compared. Using 100 partitions is considered sufficient to ensure stable CI estimates. According to [23], the most optimal and suitable number of clusters (value of k) is the smallest value for which the CI exceeds 90% of the CI values obtained from random red noise.

3. Results and Discussion

3.1 Determination of number of clusters

Fig 2 presents the CIs obtained from k-means clustering analysis for $k = 2$ to $k = 10$. The grey shading indicates the lower 90% of CI values generated from random red noise, and providing a statistical baseline. A comparison between the observed CI values and those from random red noise shows that the 850-hPa wind patterns can be effectively grouped into four distinct clusters ($k = 4$), as this value exceeds the red noise threshold. This finding suggests that the $k = 4$ partitioning captures meaningful and robust atmospheric patterns, indicating that four WTs provide an optimal representation of the synoptic-scale circulation variability over Malaysia during the Northeast Monsoon season.

Fig 2. Classifiability index (CI) for each cluster. The blue solid line indicates the CI value and the gray shading represented the one-sided 90% confidence interval of CI values generated through random noise.

3.2. General characteristics of WT patterns

In this study, each day during the study period was grouped to a specific WT based on similarities in their atmospheric circulation patterns. Days exhibiting similar atmospheric characteristics were grouped into the same cluster, ensuring that each WT represents a coherent set of circulation features. The identified WTs are illustrated in Fig 3 as composite representations of low-level wind patterns at the 850-hPa level. These composites describe and summarize the spatial variability and structure of the dominant weather patterns.

Fig 3. Mean wind speed (shading) and 850-hPa wind vectors for each of the four WTs.

Figure 3a illustrates WT1, which is characterized by the simultaneous occurrence of two key synoptic-scale features during the Northeast Monsoon: a cold surge and the Borneo Vortex. The cold surge, as identified by [38] is marked with the strengthened northeasterly winds over northern South China Sea extending toward Borneo. This cold surge coincides with the development of a counterclockwise circulation over the South China Sea, centered near western Borneo, which likely represents the Borneo Vortex. The formation of the Borneo Vortex is attributed to wind-terrain interactions and the conservation of potential vorticity during the Northeast Monsoon [5, 16, 20]. This simultaneous occurrence is likely due to the cold surges intensify northeasterly winds, increasing relative vorticity and mass convergence, which in turn promotes the formation of the Borneo Vortex. In fact, studies suggest that the Borneo Vortex develops due to the high vorticity background created by the horizontal cyclonic shear of the cold surge [8, 17]. As a result, these two phenomena frequently co-occur, reinforcing each other's development [20, 39]. Additionally, the observed cyclonic circulation aligns with well-documented Borneo Vortex formation regions, particularly along the western Borneo. Over the past 20 seasons, more than 120 vortex centers have been recorded in this area, particularly around 1.5°N, 111°E [8]. Furthermore, [7] further reported that when a Borneo Vortex coincides with a Cold Surge, it typically forms in the western Borneo region, which aligns with the location of the Borneo Vortex observed in this WT.

A notable characteristic of WT2 (Figure 3b) is the occurrence of a single cold surge event, which is weaker than WT1 and does not lead to the formation of a Borneo Vortex. This WT represents a weakening cold surge where northeasterly winds intensify, but remain weaker than those in a typical cold surge event. As the wind crosses the equator, it undergoes an eastward deflection due to the planetary vorticity gradient. This deflection is further modified by the interaction of the wind with topographic features which cause additional blocking and deflection effects [40].

Observations in WT3 (Figure 3c) show the occurrence of a large Borneo Vortex over northern Borneo, located over South China Sea. This Borneo Vortex is accompanied by a broad belt of westerly winds extending zonally across southern Malaysia, between 4°N and 3°S. Studies have shown that the Borneo Vortex in WT3 is situated in one of its most common formation regions, which is slightly north of the equator along the eastern coast of Borneo, near 112.5°E and 7.5°N [16]. According to [33] the Borneo Vortex near the South China Sea is formed because of the interaction between near-equatorial westerlies which is deflected by the topography of Kalimantan, and the easterly flow originating from Vietnam. Additionally, its development may involve tropical storms crossing the southern Philippines, which propagate westward and interact with the northeast monsoonal flow.

WT4 (Figure 3d) initially features an intensification of winds over the northern South China Sea, followed by a weakening phase and a subsequent second intensification near the Java

Sea. This wind pattern, which characterized by winds crossing the equator near Singapore, likely represents a cross-equatorial surge. Its features are consistent with previous studies showing that cross-equatorial surges generate stronger wind anomalies than cold surges, with their influence extending from the South China Sea down to the Java Sea [41].

Lastly, a comparison was made between the WTs identified in this study and those from previous research, including [33], to enhance the interpretation of the findings. Two of the WTs from their study (see Figure 9) closely match those identified here: WT1 corresponds to their R4, and WT3 aligns with their R6. This consistency across studies strengthens the reliability of the classification and provides additional validation of the identified weather patterns.

3.3. Occurrence Frequency

The next step involves analyzing the occurrence frequency of each WT, as shown in Fig 4. Figure 4a shows the average annual occurrence frequency for each WT, providing insights into the overall prevalence of each WT throughout the study period. Figures 4b to 4e show the monthly occurrence frequencies from November to February, highlighting the seasonal variations in the distribution of WTs. The all-year average frequency distribution of WTs shows that each WT occurs on approximately 15% to 28% of the total number of days during the study period (Figure 4a). Among the four WTs, WT2 has the lowest frequency, while WT1 and WT3 occur at similar frequencies, each accounting for around 28% of the days, with WT3 occurring slightly more frequently than WT1.

Fig 4. Percentage of days assigned to each clustered WT. (a) November to February and (b–e) individual months: (b) January, (c) February, (d) November, and (e) December.

Significant intraseasonal variations in WT frequency are observed at the monthly scale. For WT1 which is associated with both cold surges and Borneo Vortex shows a pronounced increase in occurrence during the late Northeast Monsoon period, particularly in January and February. This seasonal pattern is in agreement with previous studies. For example, [42] reported that cold surges peak in January, highlighting their dominance during the latter part of the monsoon season. Similarly, [41] observed that cold surges occur most frequently in December (56.7%) and January (72.3%), further supporting the observed trend.

WT2 which represents a weakening cold surge, shows peak occurrences in November. This timing may indicate the onset of the cold surge season, which typically spans from November to February [42]. In November, cold surges are in their early stages of development and are generally weaker compared to those later in the season, which explains the peak in WT2 occurrence during this month. For WT3 which associated with Borneo Vortex occurring over South China Sea exhibits a distinct seasonal cycle. Its frequency peaks in November, gradually declines from November to January, and then increases again in February. This pattern suggests that WT3 may be influenced by both early and late phases of the Northeast Monsoon.

For WT 4 which is associated with cross-equatorial surges, gradually increases in frequency from November to January, becoming more prominent during the late monsoon season. This trend suggests that cross-equatorial surges intensify as the northeast monsoon matures, peaking toward the season’s end. While studies such as [33] and [43] identify February as the peak period for these surges, this reinforces the idea that cross-equatorial flow strengthens as the monsoon transitions toward its end.

3.4. Progression and Persistence of WTs

Fig 5 illustrates the progression between different WTs over Malaysia, while Fig 6 shows the persistence of each WT. Understanding how these patterns evolve from one day to the next offers deeper insight into the dynamics of monsoonal circulation [24]. In this study, progression is defined as the percentage of a given WT shifting to a different WT on the following day while persistence refers to the percentage of day a specific WT remains the same on the next day.

Fig 5. Progression of each WT

Fig 6. Persistence of each WTs

In terms of WT progression (Figure 5), all WTs predominantly exhibit self-persistence, indicating a strong tendency to maintain the same pattern from one day to the next. Among the transitions, WT1 most frequently evolves into WT3, followed by WT4. WT2 shows a higher likelihood of transitioning into WT4, and to a lesser extent into WT3, suggesting that the dissipation of a cold surge may be followed by the intensification of cross-equatorial flow or the development of a Borneo Vortex event. WT3 commonly transitions into either WT1 or WT4, implying that the presence of the Borneo Vortex may be followed by the cold surges or be overtaken by cross-equatorial surges. WT4, on the other hand, most often progresses into WT1, indicating that cross-equatorial surges may play a role in initiating or modulating subsequent cold surge events and Borneo Vortex activity.

Figure 6 illustrates the persistence characteristics of the WTs. In general, all WTs tends to persist for a few days to approximately one week. For the WTs that is associated with Borneo

Vortex occurrences (WT1 and WT3), persistence typically persists for around eight days, as both WT1 and WT3 exhibit a significant decline in persistence after eight and nine days respectively. This behavior aligns with the nature of the Borneo Vortex, which tends to persists for several days to over a week during each episode [7, 16]. The WT which shows a weakening cold surge (WT2) exhibit the shortest persistence, with a noticeable drop in persistence beyond seven days. According to [1] cold surges generally last from a few days to more than a week. The reduced persistence of WT2 may be due to the rapid dissipation of weak cold surges or their transition into stronger events. Finally, WT4 which represents a cross-equatorial surge, generally persists for about six days.

3.5. WTs trends

Fig 7 shows the annual frequency trends of each WT during the November–February period and shows notable variations over time. Among the four WTs, WT1 which represents the simultaneous occurrence of cold surges and Borneo Vortex exhibits a statistically significant downward trend at the 5% significance level, indicating a notable decline in the frequency of the co-occurrence of cold surges and the Borneo Vortex during the study period. In contrast, the other WTs display weak upward trends. These include WT2, which is associated with weakening cold surges; WT3, which represents Borneo Vortex events; and WT4, which is linked to cross-equatorial surges.

Fig 7. Annual frequency of occurrence for each WT with estimated linear trends (black lines).

The observed increase in the frequency of WT 3, which is associated with the Borneo Vortex, is consistent with the findings of [19], who reported a 7% per-decade increase in Borneo Vortex occurrences from 1962 and 2007. This trend suggests a long-term enhancement in the occurrence of Borneo Vortex over the region. Additionally, the positioning of WT 3, where the Borneo Vortex is located in the central South China Sea, aligns with previous studies indicating a northward shift in the vortex's position [19]. This displacement also likely explains the decline in WT 1, as the Borneo Vortex, previously centered over western Borneo is now occurring farther north. This northward shift has important climatic implications for the region. As the Borneo Vortex moves northward into the South China Sea, its interaction with land decreases, reducing the steering effect that typically directs it toward Borneo. Consequently, the vortex system remains over the sea for extended periods, potentially contributing to an increase in occurrence of Borneo Vortex days and influencing associated rainfall over both land and ocean regions.

3.6. Relationship between WTs and Precipitation

Fig 8 shows the climatological mean of daily precipitation for each identified WT, highlighting the spatial difference in rainfall patterns under distinct synoptic circulation. This approach identifies regions that consistently experience high or low precipitation across various WTs. Meanwhile, Fig 9 shows the 99th percentile of precipitation, illustrating the intensity and spatial extent of extreme rainfall events associated with each WT.

Fig 8. Mean climatology daily precipitation over Malaysia region in each of the four WT

Fig 9. Mean 99th percentile daily precipitation over Malaysia region in each of the four WTs

WT1 (Figure 7a) is characterized by the the Borneo Vortex and a cold surge occur simultaneously, with prevailing northeasterly 850-hPa winds over the South China Sea leading to a notable increase in convective activity. This synoptic configuration results in intensified precipitation along the eastern coast of Peninsular Malaysia, as well as over western and central Borneo (Figure 8a). Furthermore, the northeastern tip of Borneo also exhibits a increase in rainfall. The intensified rainfall over western and central Borneo is attributed to the proximity of the Borneo Vortex, which enhances relative vorticity, strengthens upward motion, and promotes moisture convergence, thereby further intensifying convection in the region. This finding is consistent with [7], who reported that deep cumulus convection near the center of the Borneo Vortex is associated with intense rainfall. On the other hand, [44] showed that the co-occurrence of Borneo Vortex and cold surge may suppress convective activity over Peninsular Malaysia while enhancing convergence over Borneo. Nevertheless, the results for WT1 shows that intense rainfall continues along the east coast of Peninsular Malaysia, implying that the interaction between the cold surge and the Borneo Vortex may be modulated by specific atmospheric conditions. For example, [45] shows that Borneo Vortex during the October-March period can lead to significant precipitation increases along the east coast of the Peninsular Malaysia and Borneo region, with rainfall increases up to 20%–25% in southeastern Peninsular Malaysia. Hence, the occurrence of the Borneo Vortex enhances rainfall over both Borneo and Peninsular Malaysia. The findings in this study, which show an extension of increased rainfall further south along the east coast of Malaysia, are consistent with these observations. Besides that, the heaviest daily rainfall in WT1 aligns with areas of strong shear vorticity, high convergence, and a positive convective index, when a cold surge and Borneo Vortex occur together in other studies such as [16] and [18]. For extreme 99^{th}

percentile rainfall events, the simultaneous occurrence of a Cold Surge and Borneo Vortex produces intense precipitation along the east coast of Peninsular Malaysia, extending from northern Malaysia into southern Thailand and further southward to southern Malaysia (Figure 9a). The highest extreme rainfall is observed in Terengganu, Malaysia. The other regions experiencing extreme precipitation include the westernmost and northeastern coastal areas of Borneo.

WT 2 (Figure 7b) represents a single cold surge event, but it illustrates a weakened surge that does not fully capture the typical rainfall distribution associated with a strong cold surge. The results suggest that during a weakening cold surge, rainfall is primarily confined to the upper east coast of Peninsular Malaysia, rather than extending further south (Figure 8b). This pattern may be attributed to reduced moisture transport from the South China Sea as a result of the weaker cold surge. Additionally, substantial rainfall is observed over eastern Borneo, with the highest precipitation concentrated in northern Borneo region. This finding is consistent with [38], who demonstrated that during cold surge events, rainfall is predominantly concentrated over northern and western Borneo. Specifically, in WT2, the rainfall distribution over Borneo is notably focused in the western and central regions of Sarawak. This results aligning with [12], who reported that cold surge events contribute to heavy rainfall along the east coast of Peninsular Malaysia and western Sarawak. The 99th percentile rainfall pattern also mirrors that of WT1 (Figure 9b). However, the extent of extreme rainfall is more limited, as it does not extend into southern Peninsular Malaysia.

WT3 (Figure 7c) represents the occurrence of the Borneo Vortex over the South China Sea. In this WT, rainfall over Peninsular Malaysia's east coast is primarily concentrated in upper east coast (Figure 8c). This pattern is likely attributed to the circulation associated with the Borneo Vortex, which suppresses rainfall transported by the northeasterly monsoon winds, resulting in reduced convective activity over much of Peninsular Malaysia [16]. However, under this weather pattern, southern Thailand experiences increased rainfall. Meanwhile, rainfall over Borneo is predominantly concentrated in the eastern part of the island, as the Borneo Vortex induces low-level wind divergence and convergence toward Borneo. Notably, rainfall decreases over both Sabah and Sarawak in Malaysia, while northeastern Kalimantan experiences enhanced precipitation. Overall, above-average rainfall is observed across much of Borneo, with the most significant increases occurring in central Kalimantan. Although the Borneo Vortex is typically associated with reduced rainfall over Peninsular Malaysia, the 99th percentile rainfall distribution reveals a concentration of extreme precipitation along the east coast, particularly in the Terengganu region (Figure 9c). This suggests that, under certain conditions, the Borneo Vortex can still contribute to localized extreme rainfall events in Peninsular Malaysia.

WT 4 (Figure 7d) characterized a cross-equatorial surge, is associated with increased rainfall over eastern coast of Peninsular Malaysia, with a slight westward expansion along the coastline (Figure 8d). In Borneo, a notable increase in rainfall is observed across most of Sarawak and northeastern Kalimantan, extending southward into central Kalimantan. Although cross-equatorial surges are typically associated with drier conditions over Peninsular Malaysia [41], the present findings do not clearly exhibit such drying. Instead, they indicate a general enhancement of rainfall across Borneo, along with a localized increase in precipitation in northeastern Borneo. The 99th percentile rainfall associated with a cross-equatorial surge reveals extreme precipitation along the east coast of Peninsular Malaysia, with the highest intensities observed near the northeastern region, particularly around Terengganu. Notably, in Borneo, extreme rainfall affects a larger area compared to other weather types, especially covering most of Sarawak, with the greatest intensity recorded in the northeastern tip of the island.

3.7. Relationships between WTs and ENSO

Malaysia is strongly influenced by ENSO, with various local impacts observed during boreal winter [4, 40, 44, 46]. To better understand this influence, each WT's frequency throughout different ENSO phases is evaluated, as shown in Fig 10 . This analysis provides valuable insights into how ENSO modulates synoptic weather patterns over Malaysia, potentially affecting rainfall distribution and overall climatic variability.

Fig 10. WT frequency during various phase of ENSO

In WT 1, where the cold surge and Borneo Vortex co-occur, more during La Niña and less during El Niño years. WT 3, associated with the Borneo Vortex without a significant cold surge influence, also shows a strong relationship with ENSO. It is more frequent during La Niña years., and occurs less often during El Niño years. Hence, Borneo Vortex more during La Niña years. There is similar findings from [47] which stated that Borneo Vortex near Malaysia is significant correlated with ENSO, with a smaller number of detection during El Niño. In contrasts, WT 2, characterized by a weakening cold surge and a cross-equatorial surge is most prominent in El Niño years, and occurs less frequently in La Niña years.

4. Conclusion

Malaysia located over the equatorial region experiences significant spatial and temporal rainfall variability due to interactions between different monsoonal circulation systems. The key drivers of monsoon rainfall variability include the ENSO [3, 48], cold surges [16, 38], Borneo vortex [5, 10, 16, 17], and other synoptic-scale circulations. These interacting factors contribute to the complexity of rainfall patterns during Northeast Monsoon in Malaysia, and underscoring the need to investigate the underlying synoptic circulation pattern driving the rainfall variability. Therefore, the purpose of this study is to enhance our understanding of monsoonal synoptic circulation by classifying daily weather patterns into distinct WTs. These WTs were identified through cluster analysis using the k-means algorithm. The k-means algorithm is applied to 850-hPa wind data covering years from 1981 to 2020. By examining these WTs, we characterize different atmospheric conditions that occur throughout the Northeast Monsoon season, offering deeper insight into the synoptic circulation influencing monsoonal weather patterns. Furthermore, the frequency distribution of these WTs provides valuable information on seasonal rainfall variability. By identifying the specific WTs and their corresponding rainfall patterns, it provides a clearer understanding of the drivers of rainfall variability during the Northeast Monsoon season.

In our study, we identified four WTs that predominantly occurs during Northeast Monsoon. The results show four main WTs, each associated with an important synoptic circulation system: (i) simultaneous occurrence of a cold surge and a Borneo vortex, (ii) a weak cold surge, (iii) Borneo vortex located in northern Borneo, and (iv) a cross-equatorial surge. Notably, the research builds upon earlier work by [33] and [49], which explored the role of synoptic circulations in the region. The WTs identified in this study shows remarkable consistency with those from their research, particularly during the Northeast Monsoon, demonstrating the robustness and stability of these weather patterns. Besides that, the WTs identified in this study have a direct influence on observed rainfall patterns in Malaysia. For example, the simultaneous occurrence Borneo vortex and cold surge results in the highest rainfall, particularly over the Peninsular Malaysia's east coast and western Borneo, and cross-equatorial surges increases rainfall across north Borneo. Over time, weather patterns that show the co-occurrence of the Borneo Vortex and cold surge has shown a declining trend, likely due to the northward shift of the Borneo Vortex, while others WTs including Borneo Vortex and cross-equatorial surge has been increasing. The study highlights how these weather patterns evolve, transition between each other, and contribute to extreme rainfall events, improving understanding of regional monsoon variability.

In conclusion, this study provides a significant contribution to the understanding of Malaysia's dominant synoptic circulation patterns and the role in shaping different rainfall variability. The identification of these robust and stable WTs enhances our understanding of Northeast Monsoon dynamics and provides a framework for evaluating climate models. Amid Malaysia’s ongoing challenges arising from climate change, research like this is essential for developing strategies to manage the risks associated with extreme weather events. Furthermore, this study provides insights into the effectiveness of climate models in simulating synoptic circulation patterns in Malaysia. By comparing the observed frequency and structure of these WTs with model simulations, researchers can evaluate the accuracy of climate models in replicating real-world conditions, which is also important in many others sectors including agriculture, water resource management, and disaster risk reduction.

Acknowledgement

This work was funded by the Malaysian Ministry of Higher Education’s LRGS Grant (LRGS/1/2020/UKM-UKM/01/6/1).

Reference

1. Ramage CS. Monsoon Meteorology. New York: Academic Press. 1971:296.
2. Tangang FT, Juneng L. Mechanisms of Malaysian Rainfall Anomalies. J Clim. 2004;17(18):3616-22. doi: https://doi.org/10.1175/1520-0442(2004)017<3616:MOMRA>2.0.CO;2.
3. Juneng L, Tangang FT. Evolution of ENSO-related rainfall anomalies in Southeast Asia region and its relationship with atmosphere–ocean variations in Indo-Pacific sector. Climate Dynamics. 2005;25:337-50. doi: https://doi.org/10.1007/s00382-005-0031-6.
4. Tangang F, Farzanmanesh R, Mirzaei A, Supari, Salimun E, Jamaluddin AF, et al. Characteristics of precipitation extremes in Malaysia associated with El Niño and La Niña events. International Journal of Climatology. 2017;37:696-716. doi: https://doi.org/10.1002/joc.5032.
5. Tangang FT, Juneng L, Salimun E, Vinayachandran P, Seng YK, Reason C, et al. On the roles of the northeast cold surge, the Borneo vortex, the Madden-Julian Oscillation, and the Indian Ocean Dipole during the extreme 2006/2007 flood in southern Peninsular Malaysia. Geophys Res Lett. 2008;35(14). doi: https://doi.org/10.1029/2008GL033429.
6. Tangang FT, Juneng L, Salimun E, Sei K, Halimatun M. Climate change and variability over Malaysia: gaps in science and research information. Sains Malays. 2012;41(11):1355-66.
7. Koseki S, Koh T-Y, Teo C-K. Borneo vortex and mesoscale convective rainfall. Atmospheric Chemistry and Physics. 2014;14(9):4539-62. doi: https://doi.org/10.5194/acp-14-4539-2014.
8. Chang C-P, Wang Z, McBride J, Liu C-H. Annual Cycle of Southeast Asia—Maritime Continent Rainfall and the Asymmetric Monsoon Transition. J Clim. 2005;18(2):287-301. doi: https://doi.org/10.1175/JCLI-3257.1.
9. Johnson RH, Houze RAJ. Precipitation cloud system of the Asian monsoon. Monsoon meteorology (Chang CP, Krishnamurti TN, eds). 1987;(New York: Oxford University Press):298-353.
10. Chen T-C, Tsay J-D, Yen M-C, Matsumoto J. The Winter Rainfall of Malaysia. J Clim. 2013;26(3):936-58. doi: https://doi.org/10.1175/JCLI-D-12-00174.1.
11. Tew YL, Tan ML, Juneng L, Chun KP, Hassan MHb, Osman Sb, et al. Rapid Extreme Tropical Precipitation and Flood Inundation Mapping Framework (RETRACE): Initial Testing for the 2021–2022 Malaysia Flood. ISPRS International Journal of Geo-Information. 2022;11(7):378. doi: https://doi.org/10.3390/ijgi11070378. PubMed PMID: doi:10.3390/ijgi11070378.
12. Moten S, Yunus F, Ariffin M, Burham N, Yik DJ, Adam MKM, et al. Statistics of northeast monsoon onset, withdrawal and cold surges in Malaysia. Petaling Jaya. 2014.
13. Tan WL, Yusof F, Yusop Z. Subseasonal to multidecadal variability of northeast monsoon daily rainfall over Peninsular Malaysia using a hidden Markov model. Theoretical and Applied Climatology. 2017;129:577-86. doi: https://doi.org/10.1007/s00704-016-1795-9.
14. Supari, Tangang F, Juneng L, Cruz F, Chung JX, Ngai ST, et al. Multi-model projections of precipitation extremes in Southeast Asia based on CORDEX-Southeast Asia simulations. Environmental Research. 2020;184:109350. doi: https://doi.org/10.1016/j.envres.2020.109350.

15. Tangang F, Chung JX, Juneng L, Supari, Salimun E, Ngai ST, et al. Projected future changes in rainfall in Southeast Asia based on CORDEX–SEA multi-model simulations. Climate Dynamics. 2020;55:1247-67.
16. Chang C-P, Harr PA, Chen H-J. Synoptic Disturbances over the Equatorial South China Sea and Western Maritime Continent during Boreal Winter. Monthly Weather Review. 2005;133(3):489-503. doi: https://doi.org/10.1175/MWR-2868.1.
17. Ooi SH, Samah AA, Braesicke P. A case study of the Borneo Vortex genesis and its interactions with the global circulation. Journal of Geophysical Research: Atmospheres. 2011;116(D21). doi: https://doi.org/10.1029/2011JD015991.
18. Chen T-C, Tsay J-D, Matsumoto J. Development and Formation Mechanism of the Southeast Asian Winter Heavy Rainfall Events around the South China Sea. Part II: Multiple Interactions. J Clim. 2015;28(4):1444-64. doi: https://doi.org/10.1175/JCLI-D-14-00171.1.
19. Juneng L, Tangang FT. Long-term trends of winter monsoon synoptic circulations over the maritime continent: 1962–2007. Atmospheric Science Letters. 2010;11(3):199-203. doi: http://doi.org/10.1002/asl.272.
20. Chang CP, Liu CH, Kuo HC. Typhoon Vamei: An equatorial tropical cyclone formation. Geophys Res Lett. 2003;30(3). doi: https://doi.org/10.1029/2002GL016365.
21. Cassou C. Intraseasonal interaction between the Madden–Julian oscillation and the North Atlantic oscillation. Nature. 2008;455:523-7. doi: https://doi.org/10.1038/nature07286.
22. Fereday D, Knight J, Scaife A, Folland C, Philipp A. Cluster analysis of North Atlantic–European circulation types and links with tropical Pacific sea surface temperatures. J Climate. 2008;21:3687-703. doi: https://doi.org/10.1175/2007JCLI1875.1.
23. Michelangeli R, Vautard R, Legras B. Weather regimes: Recurrence and quasi-stationarity. J Atmos Sci. 1995;52:1237-56. doi: https://doi.org/10.1175/1520-0469(1995)052<1237:WRRAQS>2.0.CO;2.
24. Roller CD, Qian J-H, Agel L, Barlow M, Moron V. Winter weather regimes in the northeast United States. J Climate. 2016;29:2963-80. doi: https://doi.org/10.1175/JCLI-D-15-0274.1.
25. Moron V, Plaut G. The impact of El Niño–Southern Oscillation upon weather regimes over Europe and the North Atlantic during boreal winter. International Journal of Climatology: A Journal of the Royal Meteorological Society. 2003;23(4):363-79. doi: https://doi.org/10.1002/joc.890.
26. Pohl B, Camberlin P, Roucou P. Typology of pentad circulation anomalies over the Eastern Africa–Western Indian Ocean region, and their relationship with rainfall. Climate Research. 2005;29(2):111-27. doi: http://doi.org/10.3354/cr029111.
27. Moron V, Robertson AW, Qian J-H. Local versus regional-scale characteristics of monsoon onset and post-onset rainfall over Indonesia. Climate dynamics. 2010;34:281-99. doi: https://doi.org/10.1007/s00382-009-0547-2.
28. Ghil M, Robertson AW. “Waves” vs. “particles” in the atmosphere’s phase space: A pathway to long-range forecasting. Proc Natl Acad Sci USA. 2002;99:2493-500. doi: https://doi.org/10.1073/pnas.012580899.
29. Lana X, Fern Mills GÁ. Minimum sample size for synoptic weather type classification. Application to winter period data recorded on the catalan coast (North-East Spain). International journal of climatology. 1994;14(9):1051-60. doi: https://doi.org/10.1002/joc.3370140909.

30. Coleman JS, Rogers JC. A synoptic climatology of the central United States and associations with Pacific teleconnection pattern frequency. J Clim. 2007;20(14):3485-97. doi: https://doi.org/10.1175/JCLI4201.1.

31. Cassou C, Terray L, Phillips AS. Tropical Atlantic influence on European heat waves. J Climate. 2005;18:2805-11. doi: https://doi.org/10.1175/JCLI3506.1.

32. Hersbach H, Bell B, Berrisford P, Hirahara S, Horányi A, Muñoz-Sabater J, et al. The ERA5 global reanalysis. Quarterly Journal of the Royal Meteorological Society. 2020;146(730):1999-2049. doi: https://doi.org/10.1002/qj.3803.

33. Hassim ME, Timbal B. Observed rainfall trends over Singapore and the Maritime Continent from the perspective of regional-scale weather regimes. Journal of Applied Meteorology and Climatology. 2019;58(2):365-84. doi: https://doi.org/10.1175/JAMC-D-18-0136.1.

34. Funk C, Peterson P, Landsfeld M, Pedreros D, Verdin J, Shukla S, et al. The climate hazards infrared precipitation with stations—a new environmental record for monitoring extremes. Scientific data. 2015;2(1):1-21. doi: https://doi.org/10.1038/sdata.2015.66.

35. Ayoub AB, Tangang F, Juneng L, Tan ML, Chung JX. Evaluation of gridded precipitation datasets in Malaysia. Remote Sensing. 2020;12(4):613. doi: https://doi.org/10.3390/rs12040613.

36. Zakaria NAB, Tangang F, Salimun E, Amirudin AA, Xiang CJ, Juneng L, et al. Spatio-Temporal Variations and El Niño Modulation of Meteorological Droughts in Malaysia. International Journal of Climatology. 2024;44(15):5560-79. doi: https://doi.org/10.1002/joc.8652.

37. Cheng X, Wallace JM. Cluster analysis of the Northern Hemisphere wintertime 500-hPa height field: Spatial patterns. J Atmos Sci. 1993;50(16):2674-96. doi: https://doi.org/10.1175/1520-0469(1993)050<2674:CAOTNH>2.0.CO;2.

38. Lim SY, Marzin C, Xavier P, Chang C-P, Timbal B. Impacts of boreal winter monsoon cold surges and the interaction with MJO on Southeast Asia rainfall. J Clim. 2017;30(11):4267-81. doi: https://doi.org/10.1175/JCLI-D-16-0546.1.

39. Cheang BK. Synoptic features and structures of some equatorial vortices over the South China Sea in the Malaysian region during the winter monsoon of December 1973. Pure Appl Geophys. 1977;115:1303-33. doi: https://doi.org/10.1007/BF00874411.

40. Chang C-P, Lu M-M, Lim H. Monsoon convection in the Maritime Continent: Interaction of large-scale motion and complex terrain. Meteorological Monographs. 2016;56:6.1-6.29. doi: https://doi.org/10.1175/AMSMONOGRAPHS-D-15-0011.1.

41. Xavier P, Lim SY, Ammar Bin Abdullah MF, Bala M, Chenoli SN, Handayani AS, et al. Seasonal dependence of cold surges and their interaction with the madden–julian oscillation over Southeast Asia. J Clim. 2020;33(6):2467-82. doi: https://doi.org/10.1175/JCLI-D-19-0048.1.

42. Cheang BK. Short- and Long-range Monsoon Prediction in Southeast Asia: Malaysia Meteoorlogical Service; 1987.

43. Liang J, Catto JL, Hawcroft MK, Tan ML, Hodges KI, Haywood JM. Borneo Vortices in a warmer climate. npj Climate and Atmospheric Science. 2023;6(1):2. doi: https://doi.org/10.1038/s41612-023-00326-1.

44. Robertson AW, Moron V, Qian J-H, Chang C-P, Tangang F, Aldrian E, et al. The maritime continent monsoon. The global monsoon system: research and forecast. 2011:85-98. doi: https://doi.org/10.1142/9789814343411_0006.

45. Liang J, Catto JL, Hawcroft M, Hodges KI, Tan ML, Haywood JM. Climatology of Borneo vortices in the HadGEM3-GC3. 1 general circulation model. J Clim. 2021;34(9):3401-19. doi: https://doi.org/10.1175/JCLI-D-20-0604.1.
46. Chang C-P, Wang Z, Ju J, Li T. On the Relationship between Western Maritime Continent Monsoon Rainfall and ENSO during Northern Winter. J Clim. 2004;17(3):665-72. doi: https://doi.org/10.1175/1520-0442(2004)017<0665:OTRBWM>2.0.CO;2.
47. Braesicke P, See Hai O, Abu Samah A. Properties of strong off-shore Borneo vortices: a composite analysis of flow pattern and composition as captured by ERA-Interim. Atmospheric Science Letters. 2012;13(2):128-32. doi: https://doi.org/10.1002/asl.372.
48. Lau N-C, Nath MJ. Impact of ENSO on the variability of the Asian-Australian monsoons as simulated in GCM experiments. J Clim. 2000;13:4287-309. doi: https://doi.org/10.1175/1520-0442(2000)013<4287:IOEOTV>2.0.CO;2.
49. Qian J-H, Robertson AW, Moron V. Diurnal cycle in different weather regimes and rainfall variability over Borneo associated with ENSO. J Clim. 2013;26(5):1772-90. doi: https://doi.org/10.1175/JCLI-D-12-00178.1.

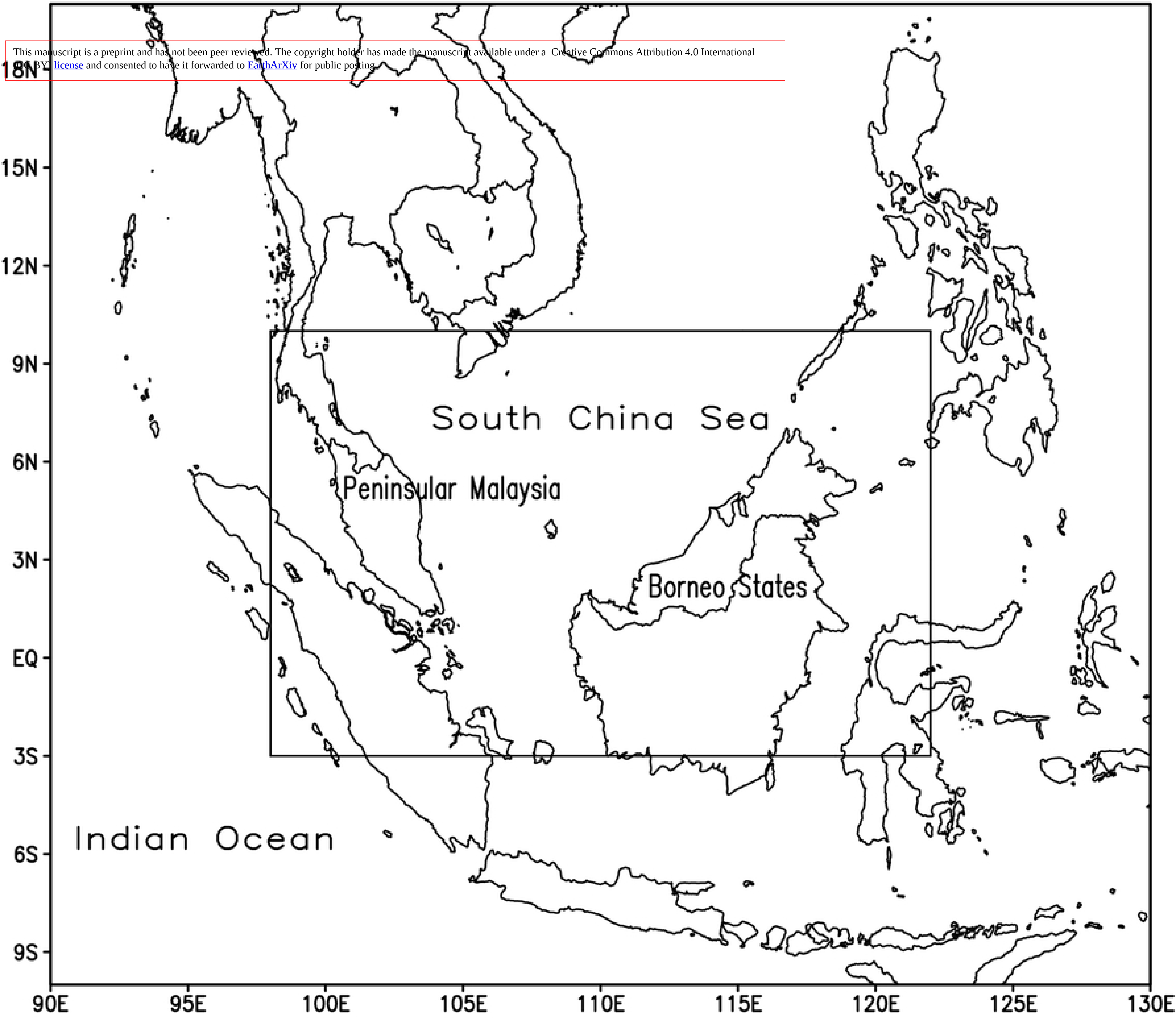

18N
15N
12N
9N
6N
3N
EQ
3S
6S
9S
90E
95E
100E
105E
110E
115E
120E
125E
130E
South China Sea
Peninsular Malaysia
Borneo States
Indian Ocean

Figure 1

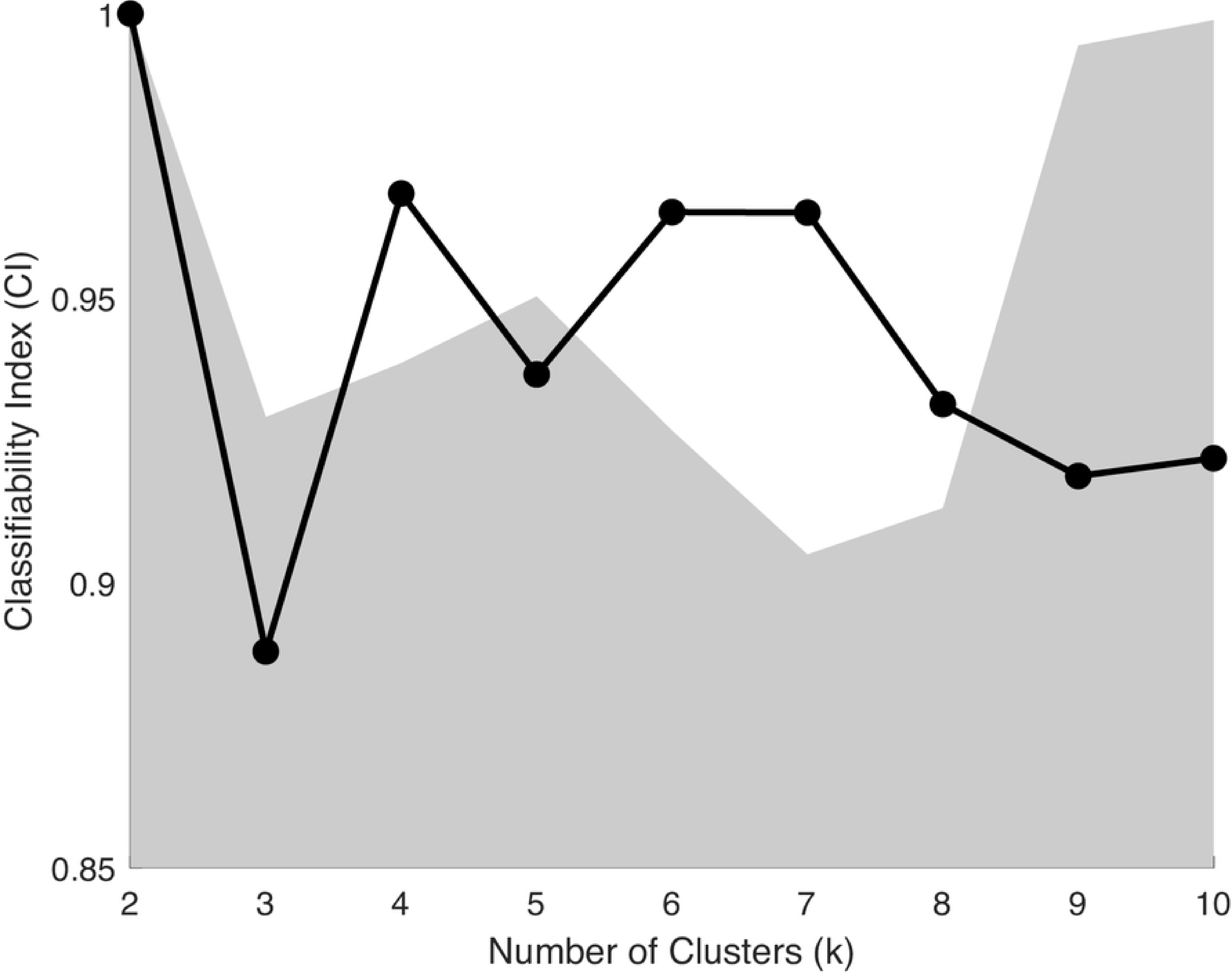

Classifiability Index (CI)
1
0.95
0.9
0.85
2
3
4
5
6
7
8
9
10
Number of Clusters (k)

Figure 2

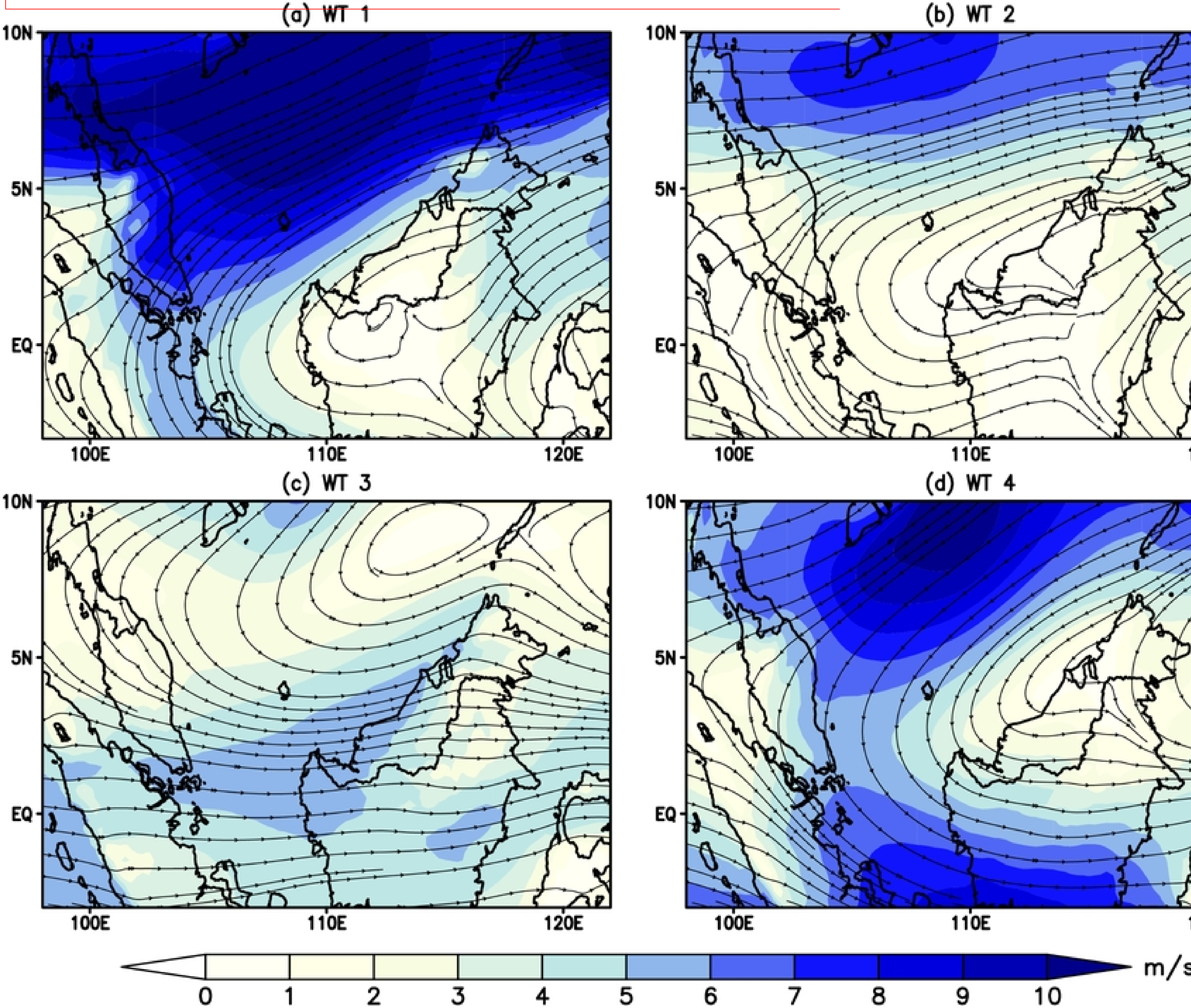

Figure 3

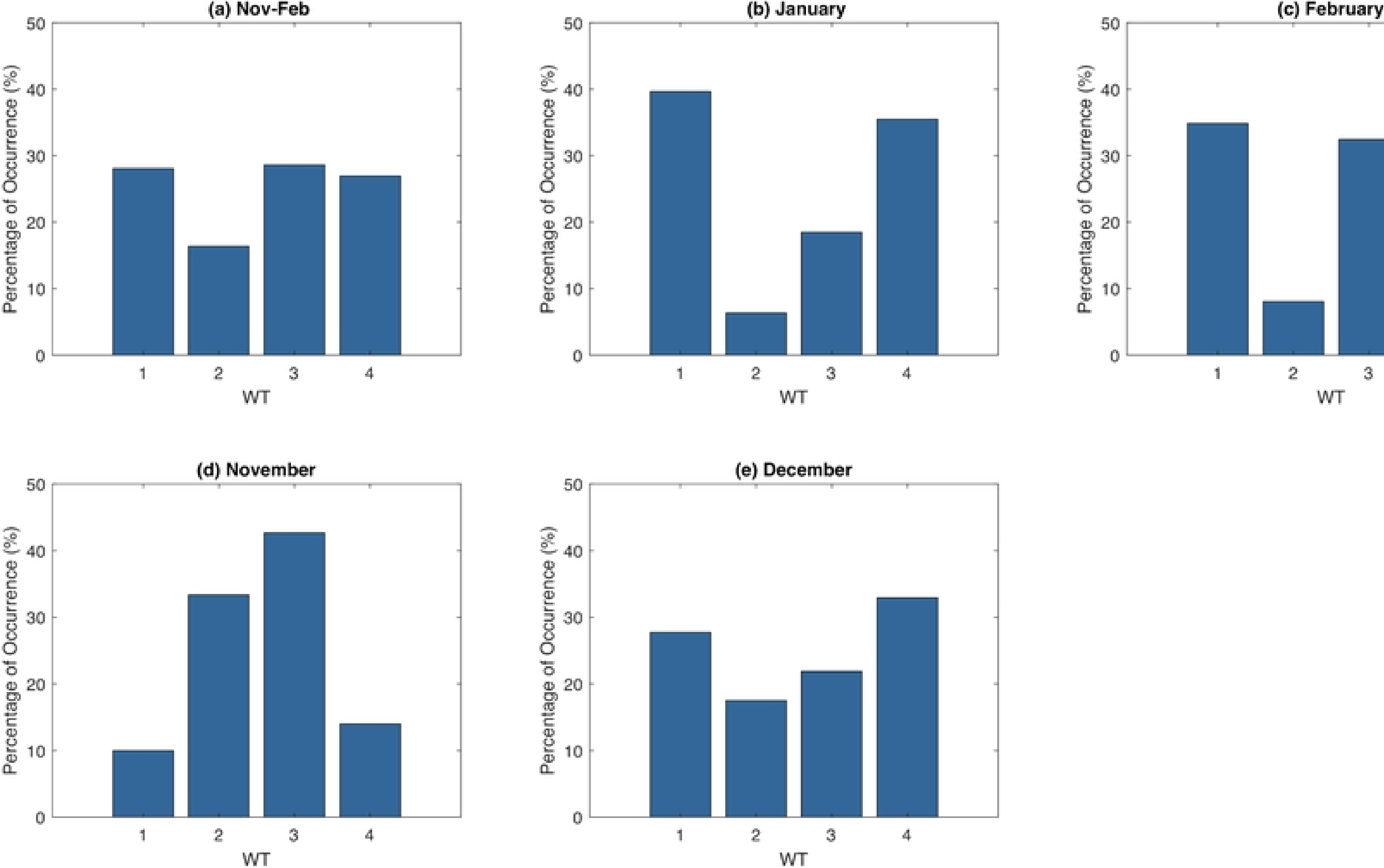

(a) Nov-Feb
(b) January
(c) February
(d) November
(e) December
Percentage of Occurrence (%)
WT
0
10
20
30
40
50
1
2
3
4

Figure 4

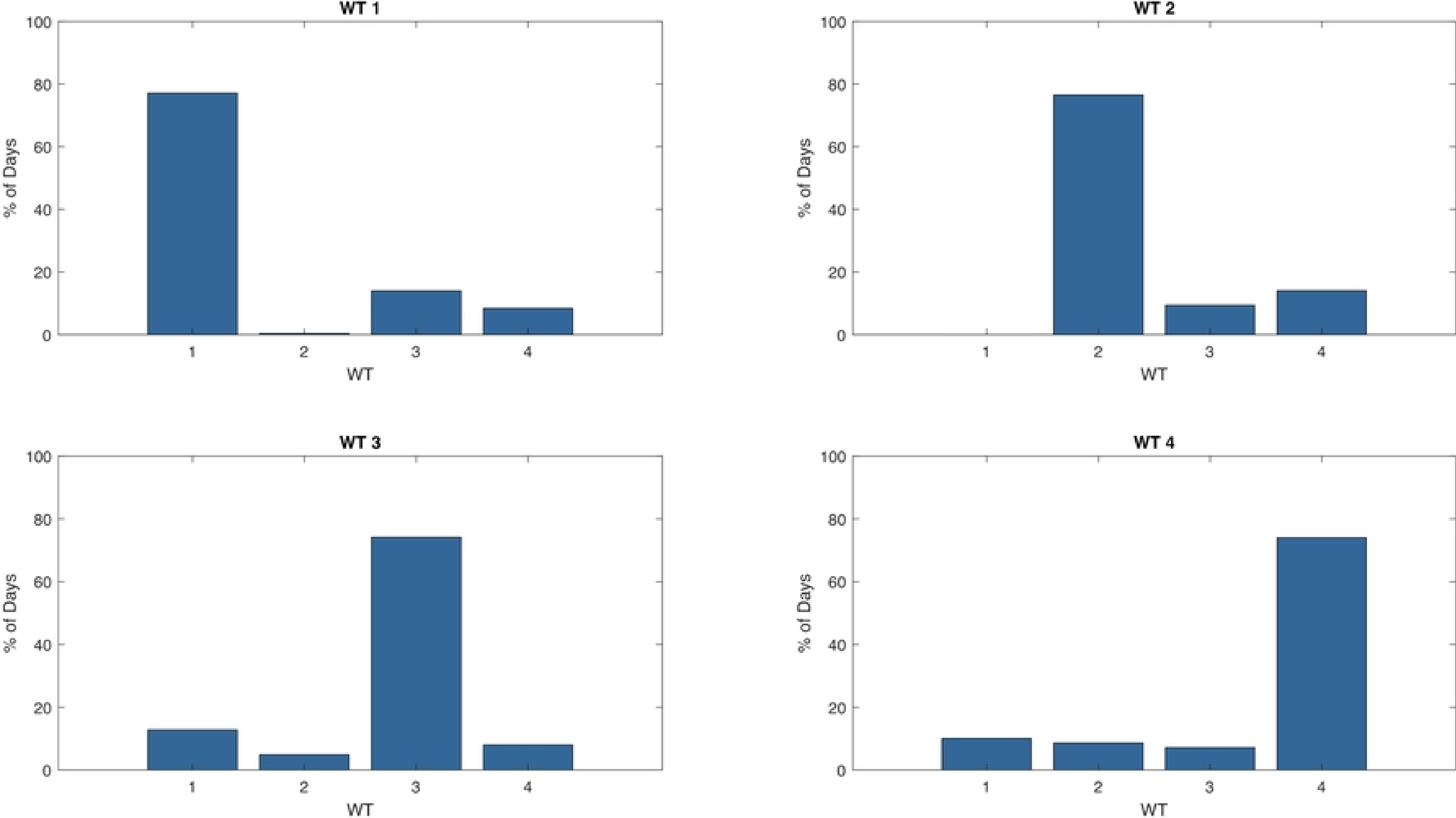

Figure 5

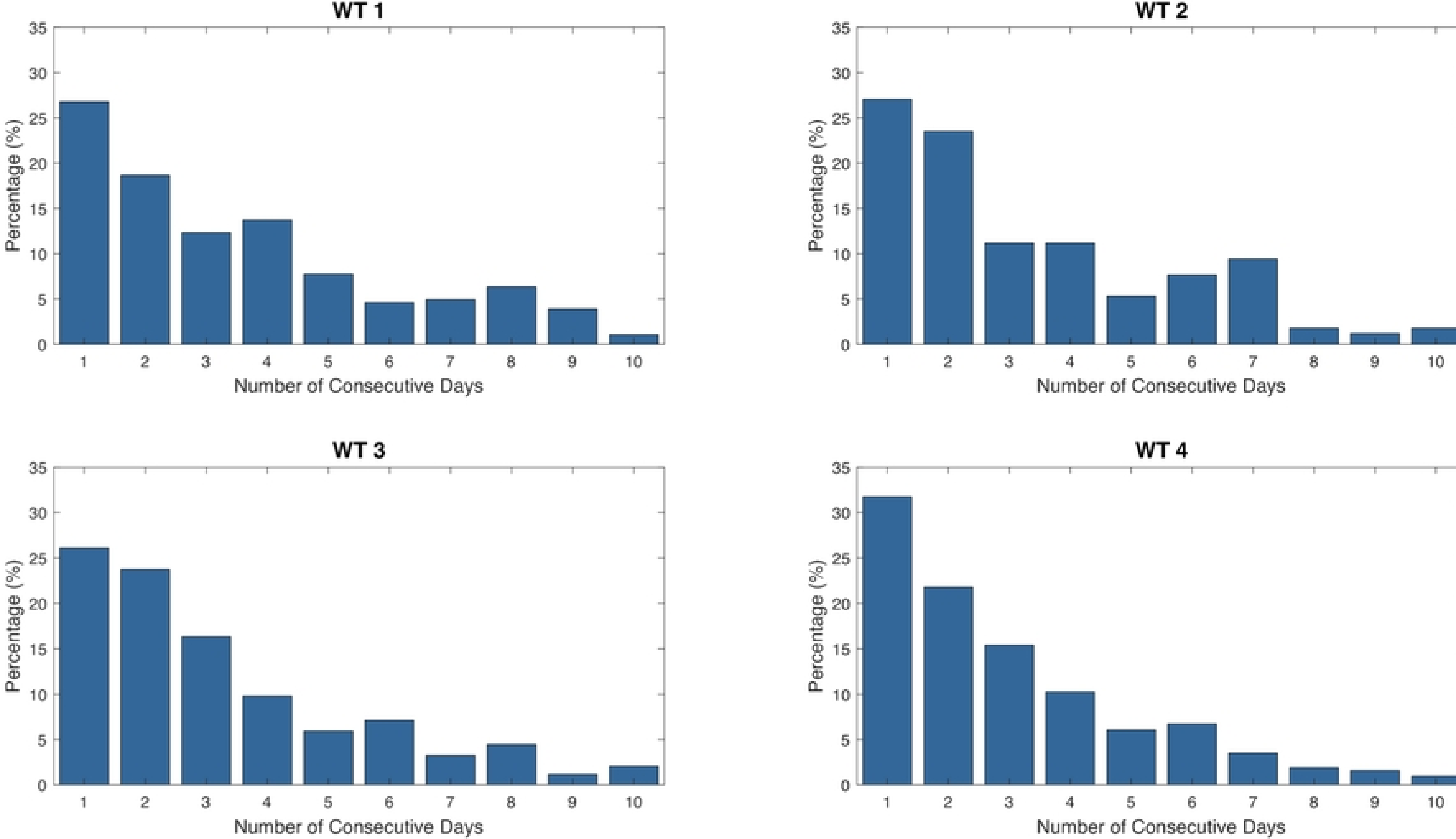
WT 1
WT 2
WT 3
WT 4
Percentage (%)
Number of Consecutive Days
0
5
10
15
20
25
30
35
1
2
3
4
5
6
7
8
9
10

Figure 6

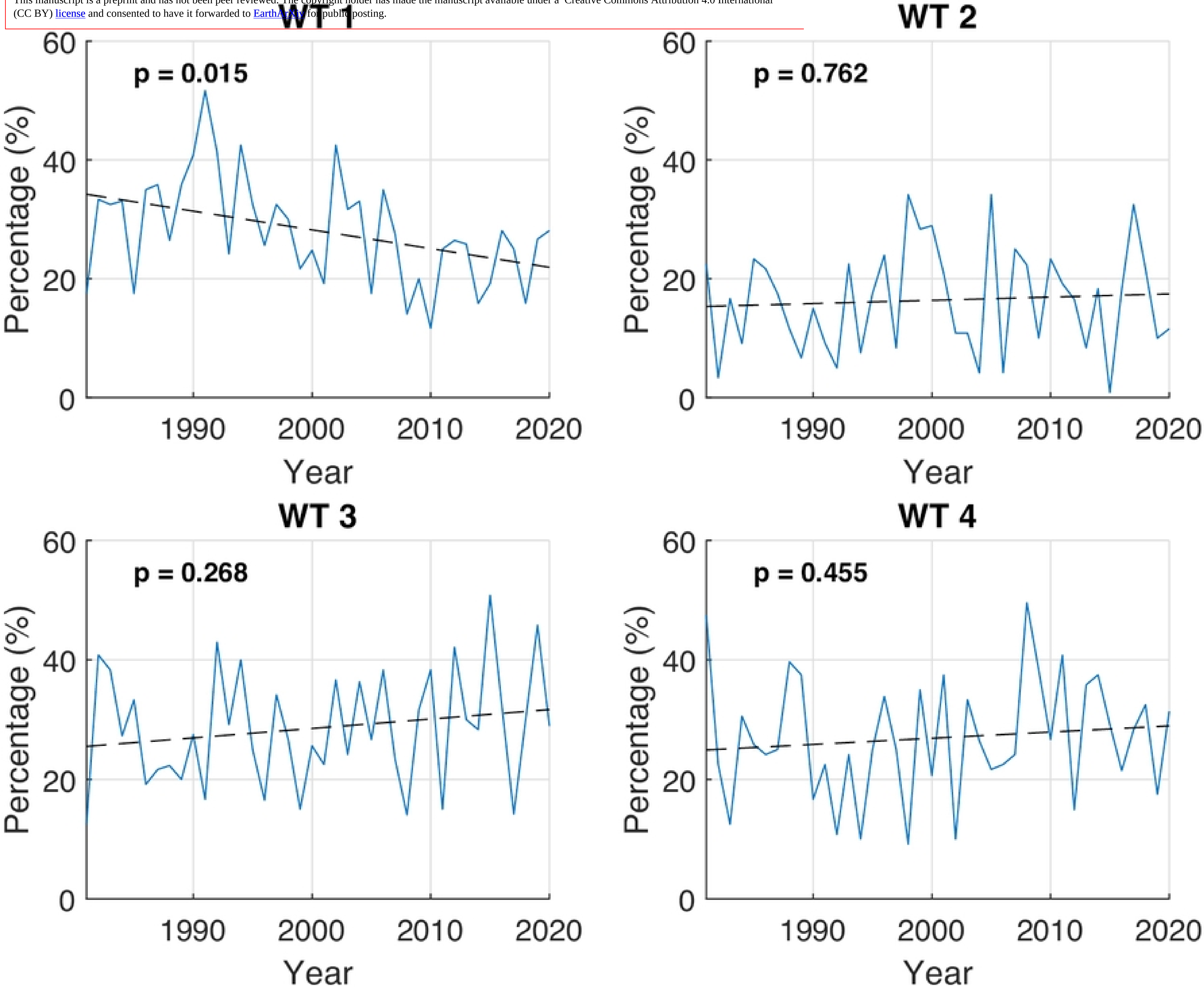
WT 1
p = 0.015
WT 2
p = 0.762
WT 3
p = 0.268
WT 4
p = 0.455
Percentage (%)
Year
0
20
40
60
1990
2000
2010
2020

Figure 7

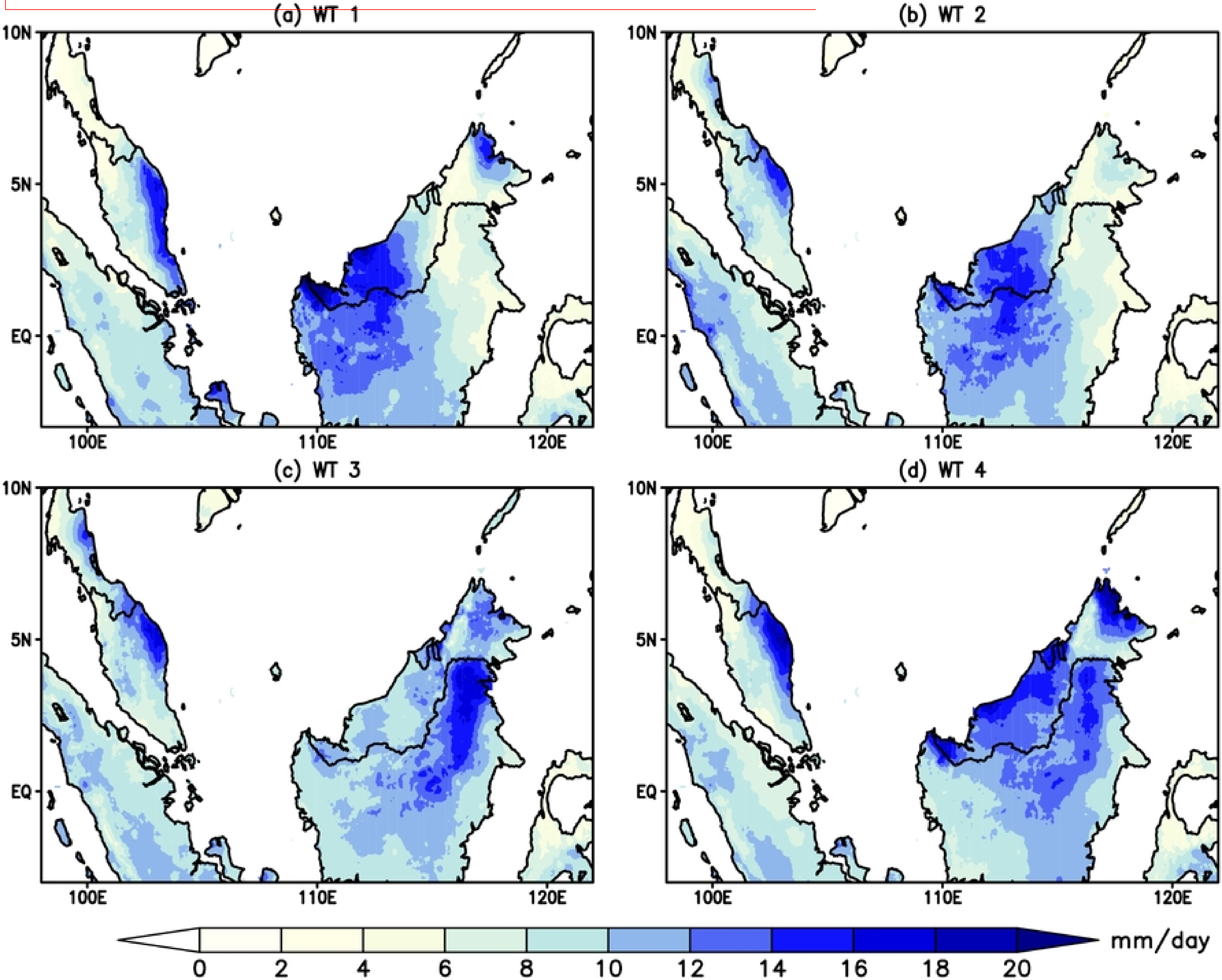
(a) WT 1
(b) WT 2
(c) WT 3
(d) WT 4
10N
5N
EQ
100E
110E
120E
0
2
4
6
8
10
12
14
16
18
20
mm/day

Figure 8

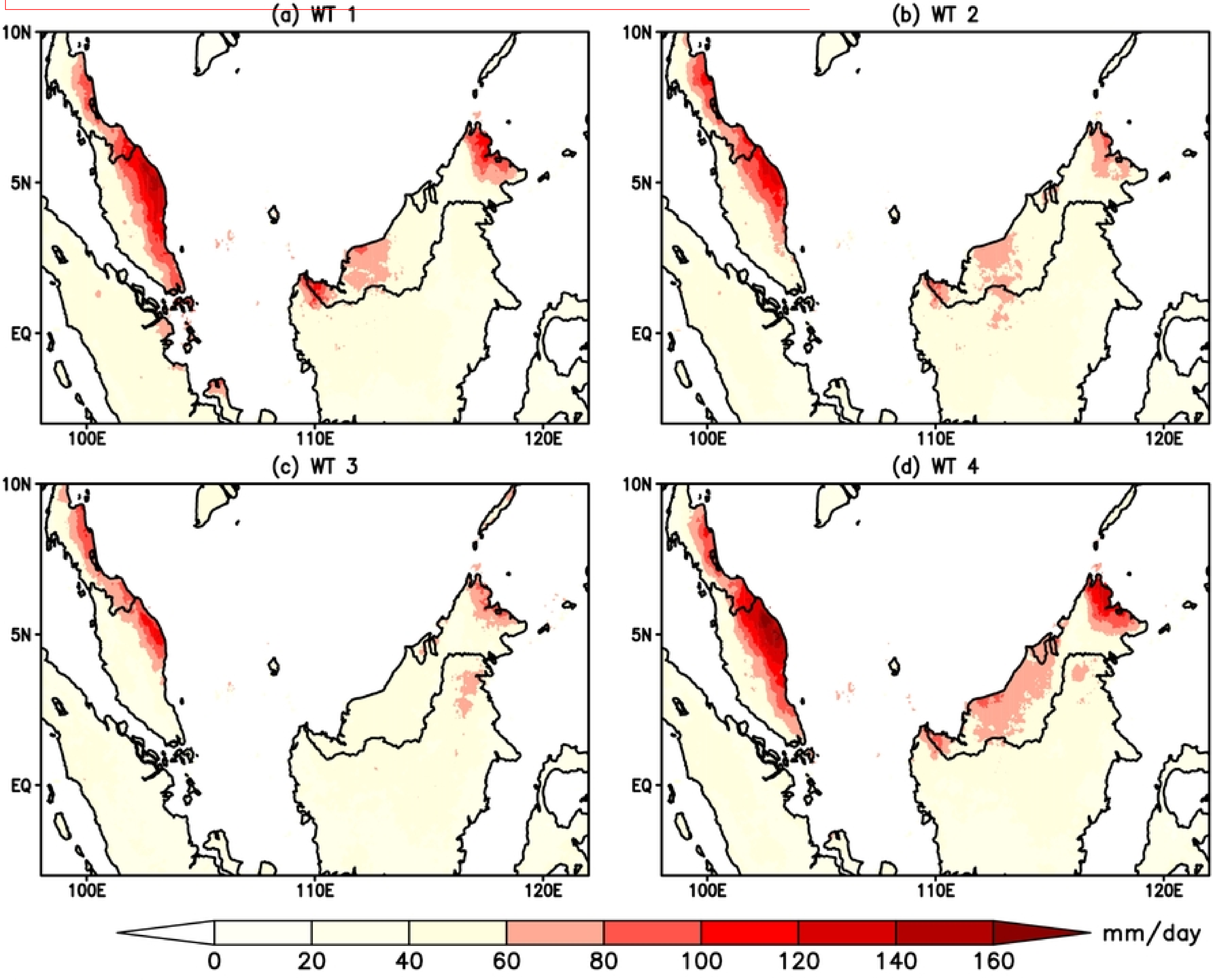

(a) WT 1
(b) WT 2
(c) WT 3
(d) WT 4
10N
5N
EQ
100E
110E
120E
0
20
40
60
80
100
120
140
160
mm/day

Figure 9

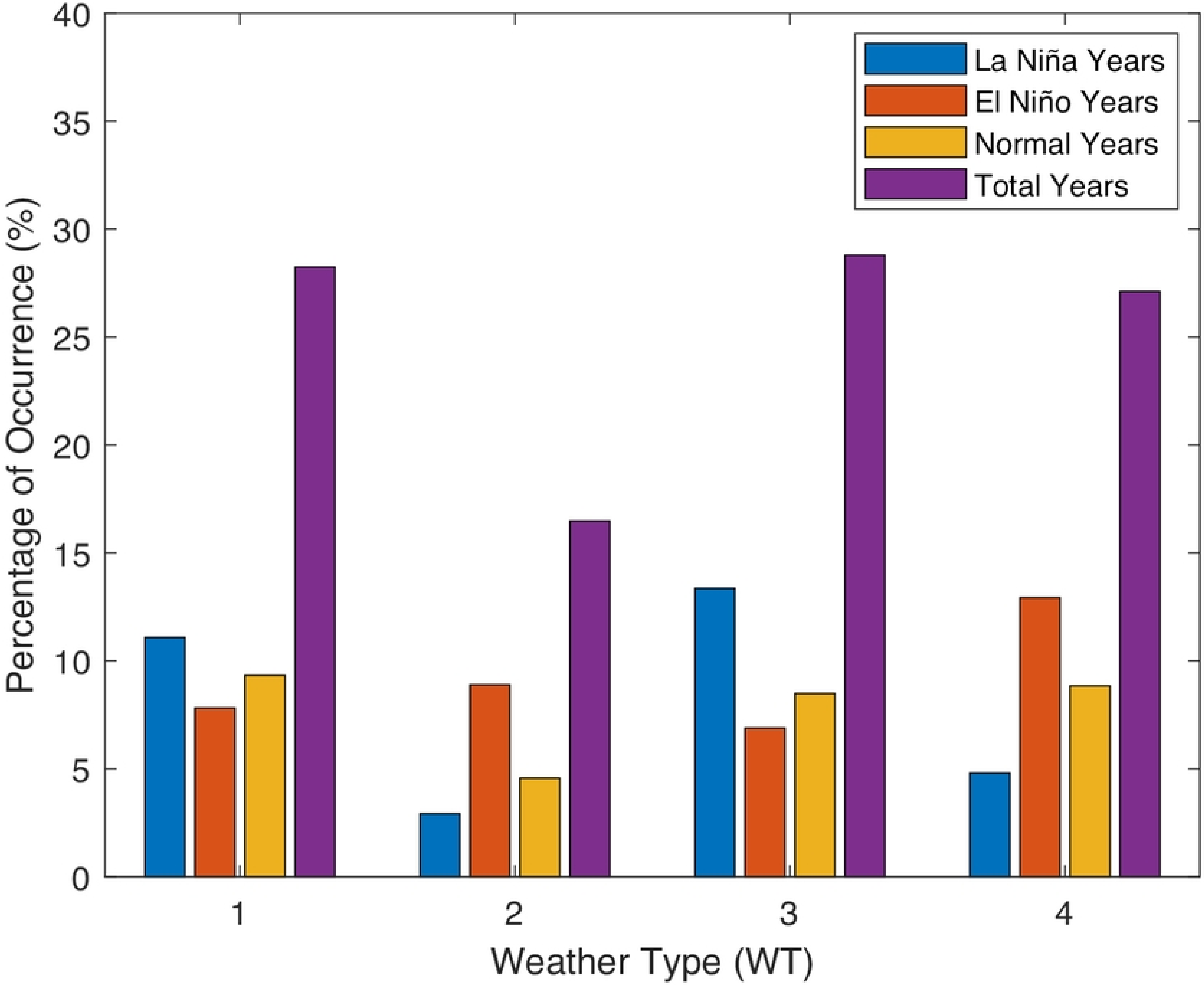

La Niña Years
El Niño Years
Normal Years
Total Years
Percentage of Occurrence (%)
0
5
10
15
20
25
30
35
40
1
2
3
4
Weather Type (WT)

Figure 10